Journal of Coordination Chemistry, 2014
Vol. 67, No. 2, 300–314, http://dx.doi.org/10.1080/00958972.2014.880784

Taylor & Francis
Taylor & Francis Group

Synthesis, crystal structure, DNA cleavage properties, and protein binding activities of an unsymmetrical dinuclear copper(II) complex

JING LU†‡§, JUN-LING LI†‡§, QIAN SUN†‡§, LIN JIANG†‡§, BI-WEI WANG†, WEN GU†‡§, XIN LIU*†‡§, JIN-LEI TIAN*†‡§ and SHI-PING YAN†‡§

†Department of Chemistry, Nankai University, Tianjin, PR China
‡Tianjin Key Laboratory of Metal and Molecule Based Material Chemistry, Tianjin, PR China
§Key Laboratory of Advanced Energy Materials Chemistry (MOE), Tianjin, PR China

(*Received 28 October 2013; accepted 16 December 2013*)

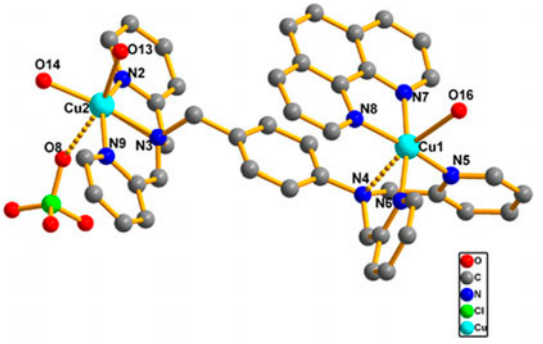

The X-ray single-crystal structure analysis shows that the complex is an unsymmetrical dinuclear species.

$[Cu_2\mathbf{L}(phen)(H_2O)_3(ClO_4)](ClO_4)_3$ {phen = 1,10-phenanthroline, **L** = 4-((bis(pyridine2-ylmethyl) amino)methyl)-N,N-bis(pyridin-2-ylmethyl)aniline} was prepared and characterized by physical chemical techniques. The X-ray single-crystal structure analysis shows an unsymmetrical dinuclear species. The interaction of the complex with calfthymus DNA (CT-DNA) was studied by various spectroscopic and viscosity measurements, which indicate that the complex can interact with CT-DNA through intercalation. In the presence of H_2O_2, the complex can cleave pBR322 DNA more efficiently and hydroxyl radicals ($HO^{\cdot}$) may serve as the major cleavage active species. Interactions of the compound with bovine serum albumin (BSA) were also investigated using UV−Vis and fluorescence spectroscopic methods. The results show that the complex quenches the intrinsic fluorescence of BSA by a static quenching mechanism.

Keywords: Unsymmetrical ligand; DNA Cleavage; Intercalation mode; A static quenching mechanism

*Corresponding authors. Email: liuxin64@nankai.edu.cn (X. Liu); tiant@nankai.edu.cn (J.-L. Tian)

1. Introduction

Metal-based pharmaceuticals have received considerable attention in medicinal inorganic chemistry, of growing significance in both therapeutic and diagnostic medicine [1–4]. The world's first anticancer drug, cisplatin (cis-$[Pt(NH_3)_2Cl_2]$), provided enormous impetus in establishing the field of medicinal inorganic chemistry in the 1960s [5]. Despite its success, platinum-based anticancer agents are non-specific, resulting in significant nephrotoxicity, neurotoxicity, and emetogenesis, limiting its application in clinical applications [6–10]. Designing other transition metal compounds that can bind and cleave double-stranded DNA under physiological conditions to overcome the toxicity and side effects of platinum compounds is a major goal.

Copper as an essential element for most organisms plays an important structural and catalytic role in a number of biological pathways [11]. Copper complexes are regarded as a potential alternative to the observed cytotoxicity in a variety of cancer cell lines [12–14]. Many copper(II) complexes have been reported to efficiently cleave DNA by oxidative, hydrolytic, photolytic, or electrolytic mechanisms. In particular, DNA cleavage by copper complexes containing poly-pyridyl ligands and their derivatives has been extensively studied [12, 15, 16].

As considerable attention has been paid to interactions of transition metal complexes with DNA, there is interest in analysis of drug–protein interactions that affect the apparent distribution volume and their elimination rate properties of drugs. Serum albumin is the major protein constituent of blood plasma with important physiological functions, such as storage and transport of endogenous and exogenous metabolites of small molecule drugs [17, 18]. Therefore, interactions of metal complexes with bovine serum albumin (BSA) receive more and more attention in pharmaceutical engineering and pharmacokinetics. Due to its structural homology with human serum albumin, BSA is the most extensively studied serum albumin [19–21]. This supports the value of studying the interaction behavior of metal complexes with BSA protein, while evaluating their anticancer properties.

Previously, we synthesized several copper complexes of 1,4-tpbd (N,N,N′,N′-tetrakis-(2-pyridylmethyl)benzene-1,4-diamine), which exhibited efficient DNA cleavage activity [22]. As continuation of our previous studies, we have been interested in exploring an unsymmetrical ligand and obtained a dinuclear copper(II) complex, and investigated its DNA cleavage activity and protein binding activity.

2. Experimental setup

2.1. *Materials*

Caution! Perchlorate salts of metal complexes are potentially explosive and therefore should be prepared in small quantities.

L was synthesized according to a previously reported procedure [23]. Chemicals and solvents were purchased from commercial sources and used as received. Plasmid pBR322 DNA, agarose, ethidium bromide (EB), calfthymus DNA (CT-DNA), BSA, and stock solutions of copper(II) complexes (1.0×10^{-3} M in CH_3CN) were stored at 4 °C and prepared at required concentrations for all experiments. Tris–HCl and phosphate buffer solutions were prepared using ultrapure water (18 MΩ cm).

2.2. *Measurements*

Elemental analyses for C, H, and N were obtained on a Perkin-Elmer analyzer model 240. Infrared spectroscopy as KBr pellets was performed on a Bruker Vector 22 FT-IR spectrophotometer from 4000 to 400 cm^{-1}. Electronic spectra were measured on a JASCO V-570 spectrophotometer. Fluorescence spectral data were obtained on a MPF-4 fluorescence spectrophotometer at room temperature. Viscosity measurements were carried out on an Ubbelodhe viscometer maintained at a constant temperature (37.0 ± 0.1 °C) in a thermostated water bath. The Gel Imaging and documentation DigiDoc-It System were assessed using Labworks Imaging and Analysis Software (UVI, UK).

2.3. *Synthesis of the complex*

2.3.1. Preparation of L. A solution of K_2CO_3 (6.98 g, 50.5 mM) in water (14 mL) was slowly added to a stirred solution of 2-(chloromethyl)pyridine hydrochloride (11.68 g, 71.2 mM) in water (9 mL) and 4-aminobenzylamine dihydrochloride (2.95 g, 14.8 mM) in ethanol (21 mL). To the above reaction mixture, 6 mL aqueous solution of sodium hydroxide (0.01 M) was added dropwise under nitrogen. After stirring for seven days in the dark at room temperature, an oily gum was formed and then extracted with dichloromethane (3 × 25 mL), and then the organic phases were combined and dried over $MgSO_4$. Most of the solvent was evaporated under reduced pressure and the remaining crude product was re-dissolved in absolute ethanol (Yield: 30.8%) (scheme 1).

2.3.2. Synthesis of $[Cu_2L(phen)(H_2O)_3(ClO_4)](ClO_4)_3$. This complex was prepared by the addition of an ethanol (10 mL) solution of **L** (0.2 mM) and 1,10-phenanthroline (0.2 mM, 0.0396 g) to an aqueous solution of $Cu(ClO_4)_2·6H_2O$ (0.4 mM, 0.1482 g) and then refluxed for 3–4 h. The solution was cooled to room temperature, filtered, and allowed to stand for evaporation at room temperature. After several days, blue block crystals suitable

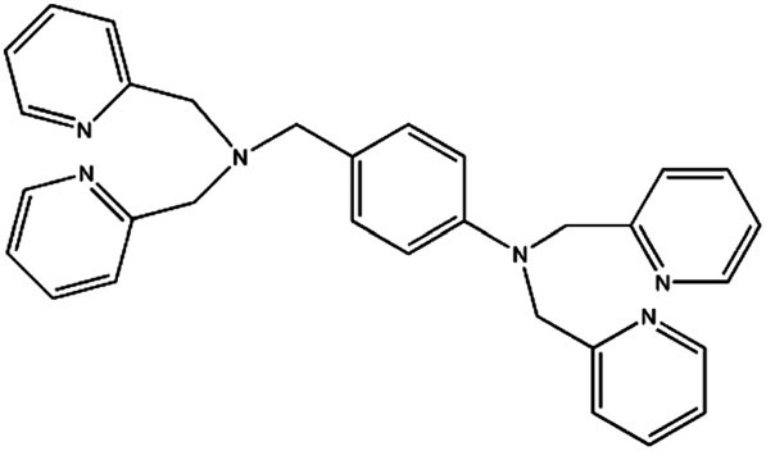

Scheme 1. **L.**

Table 1. Crystal data and structure refinement for the complex.

Compound	Complex **1**
Chemical formula	$C_{43}H_{44}Cl_4Cu_2N_8O_{19}$
Formula mass	1245.74
Crystal system	Triclinic
a/Å	9.7892(5)
b/Å	16.1191(6)
c/Å	16.9868(6)
α/°	106.583(3)
β/°	93.670(4)
γ/°	91.180(4)
Unit cell volume/Å^3	2561.53(19)
Temperature/K	127(2)
Space group	*P*
Z	2
No. of reflections measured	17,370
No. of independent reflections	8928
R_{int}	0.0242
Final R_1 values ($I > 2\sigma(I)$)	0.0844
Final w$R(F^2)$ values ($I > 2\sigma(I)$)	0.2274
Final R_1 values (all data)	0.1048
Final w$R(F^2)$ values (all data)	0.2439

for X-ray crystallography were obtained (Yield ca. 46% (based on the copper salt)). Elemental analysis (%) : Calcd for $C_{43}H_{44}Cl_4Cu_2N_8O_{19}$: C, 41.46; H, 3.56; N, 8.99. Found: C, 41.38; H, 3.62; N, 8.87. FT-IR (KBr, *v*, cm^{-1}): 3238 m (ν_{N-H}), 2027 m, 1636 *versus* 1617 s, 1144 m, 1119 m, 625 s, 484 m.

2.4. *X-ray crystallographic studies*

Determination of the unit cell and data collection for the complex were performed on a SuperNova single-crystal diffractometer equipped with graphite-monochromated Mo-Kα radiation ($\lambda = 0.71073$ Å) using the ω-scan technique. The structure was solved by direct methods (SHELXS-97) and refined with full-matrix least-squares on F^2 using SHELXL-97 [24, 25]. Hydrogens were added theoretically, riding on the concerned atoms and refined with fixed thermal factors. Details of the crystallographic data and structure refinement parameters are summarized in table 1. We collected the crystal data several times at low or room temperature and obtained better quality data with the low R_{int} value, but the final R_1 value is slightly higher due to structural disorder associated with the pyridine and ClO_4^-.

2.5. *DNA binding studies*

The CT-DNA stock solution was prepared by diluting DNA in Tris–HCl/NaCl buffer (pH 7.2, 5 mM Tris–HCl, 50 mM NaCl) and kept at 4 °C for no longer than a week. The compound was dissolved in ultrapure water (18 MΩ cm) and acetonitrile. The DNA binding experiments were performed at room temperature in Tris–HCl/NaCl buffer (50 mM Tris–HCl/1 mM NaCl buffer, pH 7.2) using an acetonitrile (CH_3CN) solution of the complex. A solution of CT-DNA in the buffer (pH 7.2) gave a ratio of UV absorbance of about 1.8–1.9 at 260 and 280 nm, indicating that the DNA was sufficiently free of protein [26]. The DNA

concentration per nucleotide was determined by absorption spectroscopy using the molar extinction coefficient value of 6600 M^{-1} cm^{-1} at 260 nm [27].

Absorption titration experiments were performed by maintaining the concentration of the complex (25 μM), while gradually increasing the concentration of DNA (0−150 μM). The absorption was recorded after each addition of CT-DNA. Fluorescence measurements were made by using a Varian Cary Eclipse spectrofluorometer. For competitive binding experiments, the complex was added to the CT-DNA solution treated with EB (2.4 μM EB and 48 μM CT-DNA) for 30 min. The samples were excited at 510 nm and emission spectra were recorded at 520–800 nm. The experiments were carried out by adding a certain amount of a solution of the complex step by step to the EB-DNA solution. The influence of the addition of the complex to the EB-DNA complex was obtained by recording the variation of the fluorescence emission spectra with excitation at 510 nm and emission at 602 nm. Before the emission spectra were recorded, the complex-DNA solutions were incubated at room temperature for 5 min to complete the reaction.

Viscosity measurements were carried out on CT-DNA by varying the concentration of the complex in 5 mM Tris–HCl/50 mM NaCl buffer (pH 7.2) using an Ubbelodhe viscometer maintained at 37.0 ± 0.1 °C in a thermostated water bath. Flow time was measured with a digital stopwatch, each sample was measured thrice and an average flow time was calculated.

2.6. *DNA cleavage and mechanism studies*

DNA cleavage experiments were done by agarose gel electrophoresis, which was performed by incubation at 37 °C as follows: pBR322 DNA (100 ng/μL) in 50 mM Tris–HCl/18 mM NaCl buffer (pH 7.2) was treated with the complex. The samples were incubated for 3 h and the loading buffer was added. Then, the samples were electrophoresed for 2 h at 80 V on 0.9% agarose gel using Tris–boric acid–EDTA buffer. After electrophoresis, bands were visualized by UV light and photographed. The extent of cleavage of the SC DNA was determined by measuring the intensities of the bands using the Gel Documentation System.

Cleavage mechanistic investigation of pBR322 DNA was carried out in the presence of standard radical scavengers and reaction inhibitors. The reactions were carried out by adding standard radical scavengers KI, NaN_3, SOD, and catalase to pBR322 DNA prior to the addition of the complexes. Cleavage was initiated by addition of complex and quenched with 2 μL of loading buffer. Further analysis was carried out by the above-mentioned standard method.

2.7. *Protein binding studies*

The protein binding study was performed by fluorescence quenching experiments using BSA stock solution (BSA, 1.5 mM) in 10 mM phosphate buffer (pH 7.0). A concentrated stock solution of the compound was prepared as used for the DNA binding experiments, except that phosphate buffer was used instead of a Tris–HCl buffer for all of the experiments. The fluorescence spectra were recorded at room temperature with excitation wavelength of BSA at 280 nm and the emission at 342 nm by keeping the concentration of BSA constant (30 μM). while varying the complex concentration from 0 to 50 μM. In addition, absorption titration experiments were carried out by keeping the concentration of BSA constant (15 μM), while varying the concentration of the complex from 0 to 2.5 μM.

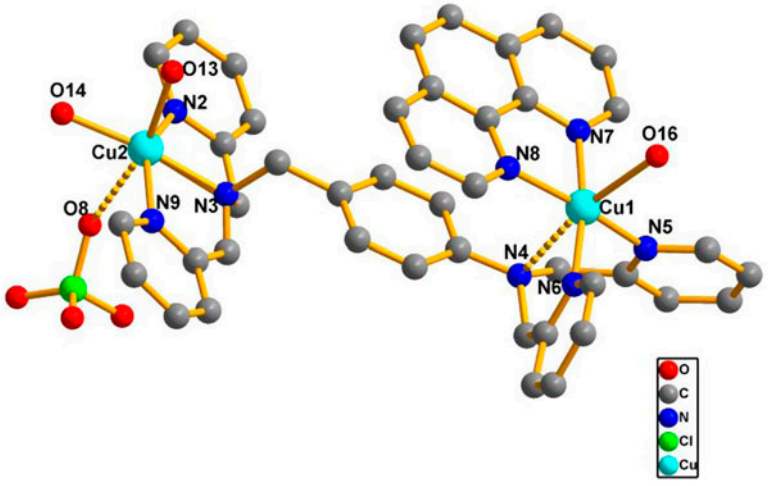

Figure 1. A view of crystal packing for the complex. Hydrogens and dissociative small molecules are omitted for clarity.

Table 2. Selected bond lengths (Å) and angles (°) for the complex.

Bond distances (Å)			
Cu(1)–N(6)	1.997(5)	Cu(1)–N(7)	2.016(5)
Cu(1)–N(5)	2.027(5)	Cu(1)–N(8)	2.040(5)
Cu(1)–O(16)	2.335(5)	Cu(1)–N(4)	2.508(5)
Cu(2)–N(3)	2.023(6)	Cu(2)–N(9)	2.083(16)
Cu(2)–O(13)	2.277(6)	Cu(2)–N(2)	1.983(7)
Cu(2)–O(8)	2.645(7)	Cu(2)–O(14)	1.957(7)
Bond angles (°)			
N(6)–Cu(1)–N(7)	171.0(2)	N(6)–Cu(1)–N(5)	92.6(2)
N(7)–Cu(1)–N(5)	92.8(2)	N(6)–Cu(1)–N(8)	91.4(2)
N(7)–Cu(1)–N(8)	81.8(2)	N(5)–Cu(1)–N(8)	167.4(2)
N(6)–Cu(1)–O(16)	98.9(2)	N(7)–Cu(1)–O(16)	87.82(19)
N(5)–Cu(1)–O(16)	95.3(2)	N(8)–Cu(1)–O(16)	95.9(2)
N(1)–Cu(2)–O(14)	90.1(4)	O(14)–Cu(2)–N(2)	102.4(4)
O(14)–Cu(2)–N(3)	172.2(3)	N(2)–Cu(2)–N(3)	77.5(3)
O(14)–Cu(2)–N(9)	106.9(6)	N(2)–Cu(2)–N(9)	147.9(5)
N(3)–Cu(2)–N(9)	71.7(5)	N(1)–Cu(2)–O(13)	88.9(3)
O(14)–Cu(2)–O(13)	83.8(3)	N(2)–Cu(2)–O(13)	99.5(3)
N(3)–Cu(2)–O(13)	104.0(2)	N(9)–Cu(2)–O(13)	96.5(4)

3. Results and discussion

3.1. *The characterization of the complex*

The structure of the complex is depicted in figure 1 and selected bond lengths and angles are listed in table 2. It crystallizes in the $P\bar{1}$ triclinic space group. As shown in figure 1, the complex consists of a dinuclear $[Cu_2\mathbf{L}(1,10\text{-phen})(H_2O)_3(ClO_4)]^{3+}$ and three ClO_4^- anions. **L** is a linker with Cu1···Cu2 distance of 9.694 Å, which is longer than the distances in other copper(II) complexes (about 8 Å) reported [22]. Compared to 1,4-tpbd reported previously, we have chosen the *p*-aminobenzylamine instead of *p*-phenylenediamine as the raw material

to synthesize our ligand. The benzyl group which increases the length of the carbon chain results in the longer distance of Cu···Cu than that of $[Cu_2(1,4\text{-tpbd})(1,10\text{-phen})_2(DMF)_2](ClO_4)_4$. In the cation, each copper is six-coordinate with N_5O donor set derived from three ligand N, two 1,10-phen N, and one coordinated water for Cu1; N_3O_3 donor set derived from three ligand N, two coordinated waters, and one perchlorate O for Cu2, forming a distorted octahedral geometry. For Cu1, N(5), N(6), N(7), and N(8) form the equatorial plane with Cu–N bond lengths from 1.997 to 2.040 Å. N(4) and O(16) occupy apical positions with Cu(1)–N(4) = 2.508 Å and Cu(1)–O(16) = 2.335 Å. For Cu2, N(2), N(3), N(9), and O(14) form the equatorial plane with bond lengths from 1.957 to 2.083 Å. O(8) and O(13) occupy apical positions with Cu(2)–O(8) = 2.645 Å and Cu(1)–O(13) = 2.277 Å. The apical bond lengths are longer than the equatorial bond lengths due to the Jahn–Teller effects in d^9 copper(II) complexes. For Cu2, a perchlorate occupies the apical position; the Cu–O bond distance observed is comparable to those observed previously [22, 28, 29].

3.2. *DNA binding modes and affinity studies*

3.2.1. Electronic absorption spectra. Electronic absorption spectroscopy is a useful method to study the binding of DNA with metal complexes. The potential binding ability of the complex to CT-DNA was studied by UV spectroscopy. Typical titration curves for the complex in the absence and presence of CT-DNA at different concentrations are given in figure 2. The complex shows characteristic charge transfer absorption bands at 200–300 nm, which are assigned as intraligand electronic spectral π–π^* transitions. With increasing concentration of CT-DNA, significant hypochromicity and a red shift are observed at the maximal peak for the complex (hypochromism of 37.8% and red shift of 11 nm), which indicates insert binding nature of the complex with CT-DNA, because intercalation would

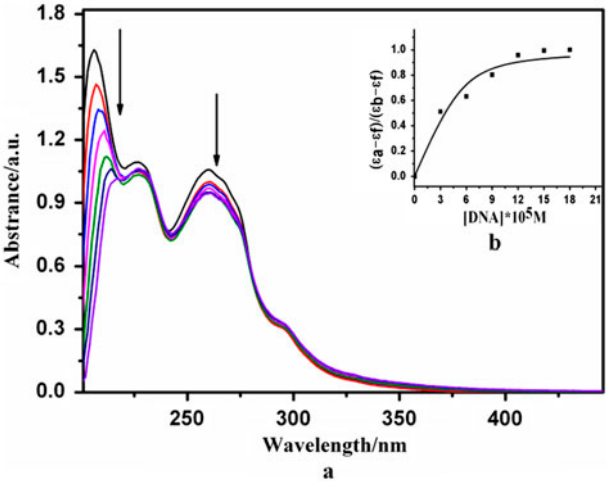

Figure 2. (a) Absorption spectra of complex (25 μM) in the absence (black line) and presence of increasing amounts of CT-DNA at room temperature in 5 mM Tris–HCl/50 mM NaCl buffer (pH 7.2). The arrow shows the absorbance changes on increasing CT-DNA concentration (b). The inset shows the plot of $(\varepsilon_a-\varepsilon_f)/(\varepsilon_b-\varepsilon_f)$ *vs.* [DNA], obtained from absorption spectral titration of the complex.

lead to hypochromism and bathochromism in UV absorption spectra owing to a strong stacking interaction between an aromatic chromophore and the base pairs of DNA [30].

The intrinsic equilibrium binding constant (K_b) and the binding site size (s) of the complex bound to CT-DNA were determined by monitoring the changes in the absorption intensity of the complex with increasing concentrations of CT-DNA. The values of K_b and s were calculated according to the equation [31, 32]:

$$(\varepsilon_a - \varepsilon_f)/(\varepsilon_b - \varepsilon_f) = (b - (b^2 - 2K_b^2 C_t[\mathrm{DNA}]/s)^{1/2})/2K_b C_t \quad (1a)$$

$$b = 1 + K_b C_t + K_b[\mathrm{DNA}]/2s \quad (1b)$$

where ε_a is the extinction coefficient observed for the charge transfer absorption band at a given DNA concentration, ε_f is the extinction coefficient of the free complex in solution, ε_b is the extinction coefficient of the complex when fully bound to DNA, C_t is the total complex concentration, and [DNA] is the DNA concentration in nucleotides.

The calculated values of K_b and s suggest a relatively strong binding of the complex to CT-DNA. The K_b value of the complex ($3.02 \times 10^5\ \mathrm{M}^{-1}$) is of the same magnitude as that of the classical intercalator EB ($K_b = 1.23\ (\pm 0.07) \times 10^5\ \mathrm{M}^{-1}$). K_b for this complex is higher than found in previous reports on copper complexes [33–35]. The better binding affinity of the present dicopper(II) complex may be attributed to more π-electrons provided by the phenanthroline ring system and aromatic ring for better stacking between the base pairs of DNA.

3.2.2. Fluorescence spectra. No luminescence is observed for the complex at room temperature, so the binding of the complex to CT-DNA was studied by a fluorescence

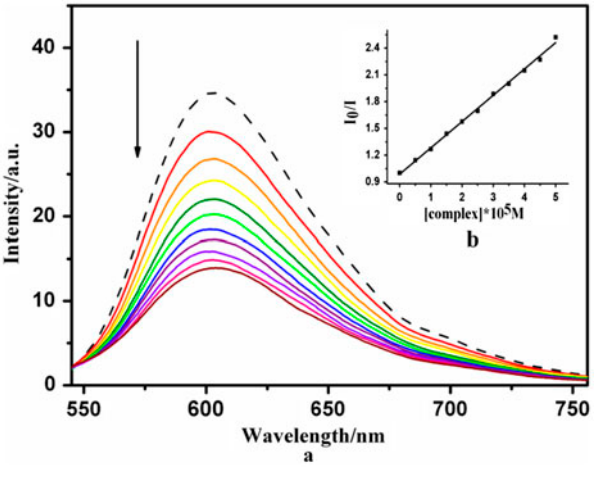

Figure 3. (a) Fluorescence emission spectra (excited at 510 nm) of the CT-DNA-EB system (2.4 μM EB, 48 μM CT-DNA) in the absence and presence of the complex with increasing the concentration from 0 to 100 μM (from top to bottom). The dashed line shows the intensity in the absence of complex (b). The fluorescence quenching curve of EB bound to DNA by the complex.

spectral method using the emission intensity of EB as a probe. EB emits intense fluorescence in the presence of CT-DNA due to its strong intercalation between the adjacent DNA base pairs [36]. A competitive binding of the complex to CT-DNA decreases the emission intensity of EB and the reduction extent of the emission intensity gives a measure to verify the DNA binding propensity of the complex.

The quenching plots (figure 3) illustrate that quenching of EB bound to CT-DNA by the complex is in agreement with the linear Stern–Volmer equation $I_0/I = 1 + K_{SV}[Q]$ (I_0 and I represent the fluorescence intensities in the absence and presence of quencher and $[Q]$ is the concentration of quencher) [37]. The values of the apparent binding constant (K_{app}) were calculated on the basis of the equation log $K_{EB}[EB] = K_{app}[complex]$, where the complex concentration was the value at a 50% reduction of the fluorescence intensity of EB and $K_{EB} = 1.0 \times 10^7\ M^{-1}$ [38], [(EB) = 2.4 μM]. The calculated K_{sv} and K_{app} values of the complex are $2.95 \times 10^4\ M^{-1}$ and $7.1 \times 10^5\ M^{-1}$, respectively ($R = 0.996470$ for eleven points), less than the binding constant of $[Cu_2(1,4\text{-tpbd})(1,10\text{-phen})_2(DMF)_2](ClO_4)_4$ ($4.86 \times 10^6\ M^{-1}$) reported by Li [22]. The K_{app} value suggests that the interaction of the copper(II) complex with DNA is a moderate intercalative mode.

3.2.3. Viscosity measurement. Viscosity measurements were carried out to further verify the interaction of the complexes with CT-DNA. In classical intercalation, the complexes result in a lengthening and stiffening of the double helix of DNA, leading to an increase in viscosity of DNA [39]. In contrast, a partial and/or non-intercalation of the ligand could result in a less pronounced effect on the viscosity [40]. The plot of relative specific viscosity $(\eta/\eta_0)^{1/3}$ *versus* [complex]/[DNA] ratio for the complex is given in figure 4. It shows that the relative viscosity of CT-DNA increased with increasing concentration of the complexes. The result suggests that the complex binds to CT-DNA through intercalation.

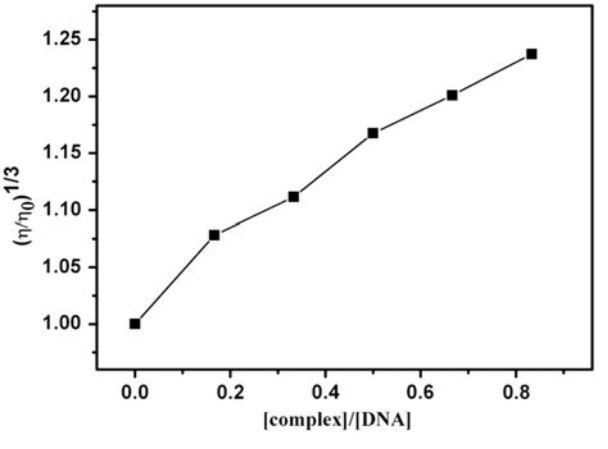

Figure 4. Effect of increasing amounts of the complex on the relative viscosity of CT-DNA at 37 (± 0.1) °C in 5 mM Tris–HCl/50 mM NaCl buffer (pH 7.2, [DNA] = 0.1 mM).

3.3. *The cleavage of pBR322 DNA*

The DNA cleavage activities of the complex have been studied using supercoiled pBR322 plasmid DNA as a substrate in a medium of 50 mM Tris–HCl/NaCl buffer (pH 7.2) in the absence of external agents under physiological conditions for 3 h. When the original supercoiled form (Form I) of plasmid DNA is nicked, an open circular relaxed form (Form II) will exist in the system and the linear form (Form III) can be found upon further cleavage. Using electrophoresis, the compact Form I migrates relatively faster, while the nicked Form II migrates slowly, and the linearized form (Form III) migrates between Forms I and II.

Concentration-dependent DNA cleavage by the complex without any external additives in natural light was performed. The result of gel electrophoretic separations of plasmid pBR322 DNA induced by increasing concentration is shown in figure 5. No obvious DNA cleavage was observed for controls in which the compound was absent (lane 6). With increasing concentration of the complex, Form I plasmid DNA is gradually converted into Form II, the complex shows poor DNA cleavage activity. At 65 μM, the complex cleaves about 83% of the plasmid to yield the nicked circular form.

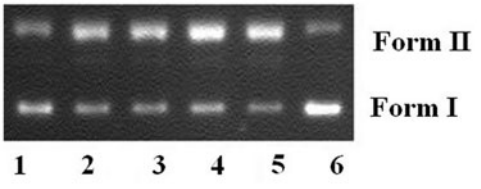

Figure 5. Agarose (1%) gel electrophoresis showing concentration-dependent cleavage of pBR322 DNA (200 ng) by complex in different condition for an incubation time of 3.0 h at 37 °C. Lane 6: DNA control; lanes 1–5: DNA + 5, 20, 35, 50, 65 μM of the complex.

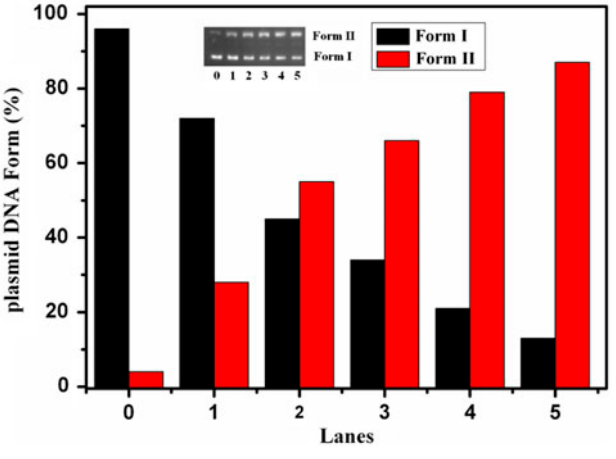

Figure 6. Agarose (1%) gel electrophoresis showing time-dependent cleavage of pBR322 DNA (200 ng) by complex in same condition at 37 °C. Lane 0: DNA control; lanes 1–5: DNA + 50 μM of complex for 0, 15, 45, 75, 135, 180 min.

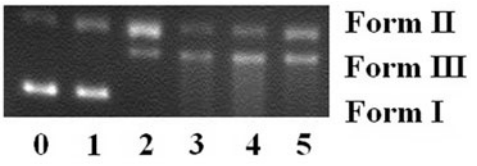

Figure 7. Agarose (1%) gel electrophoresis showing concentration-dependent cleavage of pBR322 DNA (200 ng) by complex in different condition for an incubation time of 3.0 h at 37 °C. Lane 0: DNA control; lanes 1–5: DNA + 5, 20, 35, 50, 65 μM of the complex + 0.25 mM H_2O_2.

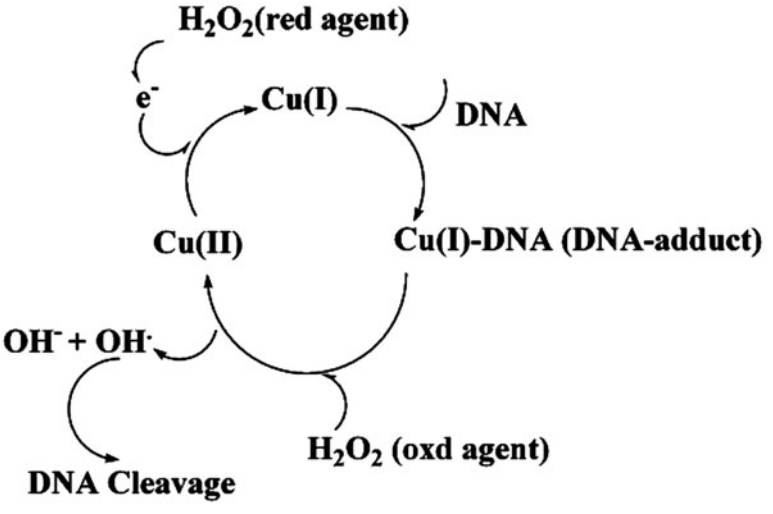

Scheme 2. Proposed mechanism for DNA cleavage by copper(II) complexes in the presence of H_2O_2.

Time-dependent cleavage of DNA by the complex was also studied under similar conditions. With increasing reaction time, the amounts of Form II increased and Form I decreased, showing that cleavage of DNA by the complex depends on reaction time (figure 6).

In the presence of H_2O_2, the DNA cleavage efficiencies of the complex exhibit remarkable increases. As shown in figure 7, in the control experiments with DNA alone and DNA with H_2O_2 alone, no DNA cleavage is observed (lane 0 and lane 1). Obviously, Form I disappeared and the linear form (Form III) can be found at 5 μM, which implies that H_2O_2 is a reductant (proposed mechanism for DNA cleavage is shown in scheme 2) [41].

3.4. *DNA cleavage mechanism*

In order to obtain further knowledge of the active chemical species responsible for the DNA damage activities by the complex, we investigated the influence of different potentially inhibiting agents including hydroxyl radical scavenger (KI), singlet oxygen quenchers (NaN_3), superoxide scavenger (SOD), hydrogen peroxide scavenger (catalase), and chelating agent (EDTA) under our experimental conditions. No obvious inhibitions were observed

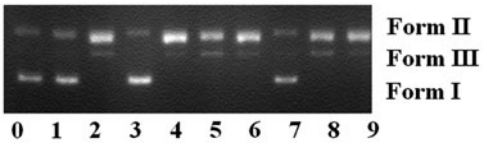

Figure 8. Agarose (1%) gel electrophoresis showing cleavage of pBR322 DNA (200 ng) by complex in different condition for an incubation time of 3.0 h at 37 °C. Lane 0, DNA control; lane 1, DNA + 0.25 mM H_2O_2; lane 2, DNA + Complex (5 μM) + 0.25 mM H_2O_2; lane 3, DNA + Complex (5 μM) + 0.25 mM H_2O_2 + KI (20 mM); lane 4, DNA + Complex (5 μM) + 0.25 mM H_2O_2 + NaN_3 (20 mM); lane 5, DNA + Complex (5 μM) + 0.25 mM H_2O_2 + SOD (20 U/mL); lane 6, DNA + Complex (5 μM) + 0.25 mM H_2O_2 + Catalase (20 U/mL); lane 7, DNA + Complex (5 μM) + 0.25 mM H_2O_2 + EDTA (10 mM); lane 8, DNA + Complex (5 μM) + 0.25 mM H_2O_2 + Methyl Green; lane 9, DNA + Complex (5 μM) + 0.25 mM H_2O_2 + SYBR.

for the complex in the presence of NaN_3 (lane 4), SOD (lane 5), and catalase (lane 6) in figure 8. These results rule out the possibility of DNA cleavage by singlet oxygen, superoxide, or hydrogen peroxide. The addition of KI (lane 3) diminishes the nuclease activity of the compounds, which indicates that the hydroxyl radical is involved in the cleavage process. The chelating agent EDTA can efficiently inhibit DNA cleavage (lane 6), indicating that the Cu(II) complex plays a key role in DNA breakage.

3.5. *Protein binding studies*

Qualitative analysis of the binding of chemical compounds to BSA is usually detected by inspecting the fluorescence spectra. Generally, the fluorescence of BSA is caused by tryptophan and tyrosine. Changes in the emission spectra of tryptophan are common in response to protein conformational transitions, subunit associations, substrate binding, or denaturation [42]. Therefore, the intrinsic fluorescence of BSA can provide considerable information on their structure and dynamics and is often utilized in the study of protein

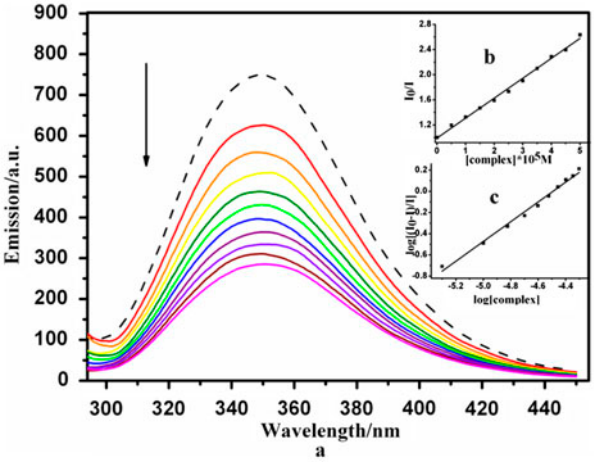

Figure 9. The emission spectrum of BSA (30 μM; λ_{exi} = 280 nm; λ_{emi} = 345 nm) in the presence of increasing amounts of complex. The dashed line shows the intensity in the absence of complex. The arrow shows the fluorescence quenching upon increasing the concentrations of the complex (a). The inset shows the Stern−Volmer plots (b) and Scatchard plots (c) of the complex with BSA.

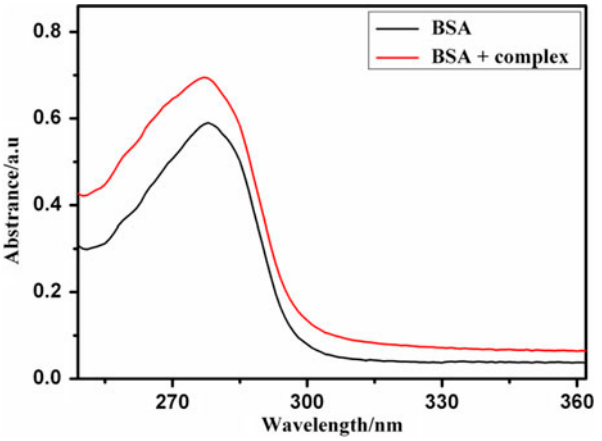

Figure 10. Absorption spectra of BSA (15 μM) and BSA with the complex (2.5 μM).

folding and association reactions. The interaction of BSA with our complex was studied by fluorescence measurement at room temperature (figure 9).

The fluorescence quenching is described by the Stern–Volmer equation and the quenching rate constant K_q was calculated with the plot of I_0/I *versus* $[Q]$. Quenching can occur by different mechanisms, which are usually classified as dynamic quenching and static quenching; dynamic quenching refers to a process in which the fluorophore and the quencher come into contact during the transient existence of the excited state. Static quenching refers to fluorophore-quencher complex formation in the ground state. A simple method to explore the type of quenching is UV−Vis absorption spectroscopy. UV−Vis spectra of BSA in the absence and presence of the compound (figure 10) show that the absorption intensity of BSA was enhanced as the compound was added, and there was a little blue shift, revealing a static interaction between BSA and the added compound due to the formation of ground state BSA-compound [43].

If it is assumed that the binding of compound with BSA occurs at equilibrium, the equilibrium binding constant can be analyzed according to the Scatchard equation [44]: $\log[(I_0 - I)/I] = \log K_{bin} + n \log[Q]$, where K_{bin} is the binding constant of the compound with DNA and n is the number of binding sites [figure 9(b) and (c)]. The K_{bin} and n values of the complex obtained are $1.53 \times 10^4\ M^{-1}$ and 0.93 ($R = 0.98983$ for ten points). The calculated value of n is 1 for the complex, indicating the existence of just a single binding site in BSA for the complex [44].

4. Conclusion

A new unsymmetrical dinuclear Cu complex, $[Cu_2\mathbf{L}(phen)(H_2O)_3(ClO_4)](ClO_4)_3$, has been synthesized and characterized by single-crystal X-ray diffraction. The interaction of the complex with CT-DNA has been investigated by UV absorption, fluorescence spectroscopy, and viscosity, and the results indicate that the complex binds to CT-DNA through intercalation. DNA cleavage studies showed that the complex exhibits DNA cleavage in the presence of H_2O_2 and hydroxyl radicals generated in the presence of the complex may act as active species for DNA scission. The ability to bind to proteins has also been explored,

which is the requisite for a drug to act as an anticancer agent for probing and targeting nucleic acids and proteins.

Supplementary material

Crystallographic data (excluding structure factors) for the structures in this article have been deposited with the Cambridge Crystallographic Data Center as supplementary publication CCDC 967951. Copies of the data can be obtained, free of charge, on application to the CCDC, 12 Union Road, Cambridge CB2 1EZ, UK.

Funding

This work was supported by the National Natural Science Foundation of China [21171101 21071083 and 21001066]; NFFTBS [No. J1103306]; Tianjin Science Foundation [No. 12JCYBJC13600].

References

[1] T. Storr, K.H. Thompson, C. Orvig. *Chem. Soc. Rev.*, **35**, 534 (2006).
[2] V. Chandrasekhar, T. Senapati. *Inorg. Chem.*, **48**, 6192 (2009).
[3] A. Hussain, S. Gadadhar, T.K. Goswami, A.A. Karande, A.R. Chakravarty. *Dalton Trans.*, **41**, 885 (2012).
[4] S. Tabassum, A. Asim, F. Arjmand, M. Afzal, V. Bagchi. *Eur. J. Med. Chem.*, **58**, 308 (2012).
[5] B. Rosenberg, L. Vancamp, J.E. Trosko, V.H. Mansour. *Nature*, **222**, 385 (1969).
[6] M.A. Fuertes, C. Alonso, J.M. Pérez. *Chem. Rev.*, **103**, 645 (2003).
[7] R. Agarwal, S.B. Kaye. *Nat. Rev. Cancer*, **3**, 502 (2003).
[8] P.U. Maheswari, S. Roy, H.D. Dulk, S. Barends, G.V. Wezel, B. Kozlevcar, P. Gamez, J. Reedijk. *J. Am. Chem. Soc.*, **128**, 710 (2006).
[9] N.J. Wheate, S. Walker, G.E. Craig, R. Oun. *Dalton Trans.*, **39**, 8113 (2010).
[10] A.I. Matesanz, C. Hernandez, A. Rodriguez, P. Souza. *Dalton Trans.*, **40**, 5738 (2011).
[11] K.J. Humphreys, K.D. Karlin, S.E. Rokita. *J. Am. Chem. Soc.*, **124**, 6009 (2002).
[12] K. Suntharalingam, D.J. Hunt, A.A. Duarte, A.J. White, D.J. Mann, R. Vilar. *Chem.-Eur. J.*, **18**, 15133 (2012).
[13] K. Abdi, H. Hadadzadeh, M. Salimi, J. Simpson, A.D. Khalaji. *Polyhedron*, **44**, 101 (2012).
[14] K. Ghosh, P. Kumar, V. Mohan, U.P. Singh, S. Kasiri, S.S. Mandal. *Inorg. Chem.*, **51**, 3343 (2012).
[15] R.N. Patel, S.P. Rawat, M. Choudhary, V.P. Sondhiya, D.K. Patel, K.K. Shukla, D.K. Patel, Y. Singh, R. Pandey. *Inorg. Chim. Acta*, **392**, 283 (2012).
[16] J. Sun, S.Y. Deng, L. Zhang, J. He, L. Jiang, Z.W. Mao, L.N. Ji. *J. Coord. Chem.*, **62**, 3284 (2009).
[17] D. Gibellini, F. Vitone, P. Schiavone, C. Ponti, M.L. Placa, M.C. Re. *J. Clin. Virol.*, **29**, 282 (2004).
[18] V. Ankita, S. Priyankar, A. Ejaz, R. Mohd, S. Naidu, K.R. Hasan. *Chirality*, **22**, 77 (2010).
[19] M. Dockal, D.C. Conter, F. Ruker. *Biol. Chem.*, **275**, 3042 (2000).
[20] N. Wang, L. Ye, F.F. Yan. *Int. J. Pharm.*, **351**, 55 (2008).
[21] S.D. Nelson. *J. Med. Chem.*, **25**, 753 (1982).
[22] D.D. Li, J.L. Tian, Y.Y. Kou, F.P. Huang, G.J. Chen, W. Gu, X. Liu, D.Z. Liao, P. Cheng, S.P. Yan. *Dalton Trans.*, 3574 (2009).
[23] T. Buchen, A. Hazell, L. Jessen, C.J. McKenzie, L.P. Nielsen, J.Z. Pedersen, D. Schollmeyer. *J. Chem. Soc., Dalton Trans.*, **15**, 2697 (1997).
[24] G.M. Sheldrick, *SHELXS-97, Program for the Solution of Crystal Structures*, University of Göttingen, Germany (1997).
[25] G.M. Sheldrick, *SHELXL-97, Program for the Refinement of Crystal Structures*, University of Göttingen, Germany (1997).
[26] J. Marmur. *J. Mol. Bio.*, **3**, 208 (1961).
[27] M.E. Reichmann, S.A. Rice, C.A. Thomas, P. Doty. *J. Am. Chem. Soc.*, **76**, 3047 (1954).
[28] K. Dhara, J. Ratha, M. Manassero, X.Y. Wang, S. Gao, P. Banerjee. *J. Inorg. Biochem.*, **101**, 95 (2007).
[29] T. Gajda, A. Jancsó, S. Mikkola, H. Lönnberg, H. Sirges. *J. Chem. Soc., Dalton Trans.*, **8**, 1757 (2002).
[30] T.K. Goswami, B.V. Chakravarthi, M. Roy, A.A. Karande, A.R. Chakravarty. *Inorg. Chem.*, **50**, 8452 (2011).
[31] M.T. Carter, M. Rodriguez, A.J. Bard. *J. Am. Chem. Soc.*, **111**, 8901 (1989).

[32] J.D. McGhee, P.H. Von Hippel. *J. Mol. Bio.*, **86**, 469 (1974).
[33] H.H. Lu, Y.T. Li, Z.Y. Wu, K. Zheng, C.W. Yan. *J.Coord. Chem.*, **64**, 1360 (2011).
[34] Y. Mei, J.J. Zhou, H. Zhou, Z.Q. Pan. *J. Coord. Chem.*, **65**, 643 (2012).
[35] Y.G. Sun, K.L. Li, Z.H. Xu, T.Y. Lv, S.J. Wang, L.X. You, F. Ding. *J. Coord. Chem.*, **66**, 2455 (2013).
[36] F.J. Meyer-Almes, D. Porschke. *Biochemistry*, **32**, 4246 (1993).
[37] J.R. Lakowicz, G. Weber. *Biochemistry*, **12**, 4161 (1973).
[38] M. Cory, D.D. McKee, J. Kagan, D.W. Henry, J.A. Miller. *J. Am. Chem. Soc.*, **107**, 2528 (1985).
[39] J.M. Kelly, A.B. Tossi, D.J. McConnell, T.C. Strekas. *Nucleic Acids Res.*, **13**, 6017 (1985).
[40] E.J. Gabbay, R.E. Scofield, C.S. Baxter. *J. Am. Chem. Soc.*, **95**, 7850 (1973).
[41] R. Loganathan, S. Ramakrishnan, E. Suresh, A. Riyasdeen, M.A. Akbarsha, M. Palaniandavar. *Inorg. Chem.*, **51**, 5512 (2012).
[42] D.S. Raja, N.S.P. Bhuvanesh, K. Natarajan. *Inorg. Chem.*, **50**, 12852 (2011).
[43] Y. Hu, Y. Ou-Yang, C. Dai, Y. Liu, X. Xiao. *Biomacromolecules*, **11**, 106 (2010).
[44] X.L. Wang, M. Jiang, Y.T. Li, Z.Y. Wu, C.W. Yan. *J. Coord. Chem.*, **66**, 1985 (2013).